Classification: Physical Sciences, Sustainability Science

Warming of the Indian Ocean threatens eastern and southern Africa, but could be mitigated by agricultural development

Chris Funk[1], Michael D. Dettinger[2], Molly E. Brown[3], Joel C. Michaelsen[1], James P. Verdin[4], Mathew Barlow[5], and Andrew Hoell[5]

[1] Climate Hazard Group, Geography Dept. University of California, Santa Barbara, CA, 93106-1120, USA.
[2] United States Geological Survey, Scripps Inst. of Oceanography, La Jolla, CA 92093-0224, USA.
[3] Science Systems and Applications, NASA-Goddard Space Flight Center. Code 614.4, Greenbelt, MD 20771, USA.
[4] United States Geological Survey, Center for Earth Resources Observation and Science, SD 57198-0001, USA.
[5] Environmental, Earth, and Atmospheric Sciences, University of Massachusetts Lowell, Lowell, MA 01854, USA.

Corresponding Author:
Chris Funk, 1629 Ellison Hall, Climate Hazard Group, Geography Department, University of California, Santa Barbara, CA, 93106-1120. Phone: 805-964-3058. Fax: 805-893-3146. chris@geog.ucsb.edu

Manuscript Information:
Number of text pages: 10 pages
Number of figures: 3 figures
Number of tables: 1 table

Word and character counts
Words in abstract: 250
Total number of characters: 38,102 characters text + 9,030 characters for figures = 47,066

Figure 1	18 cm x 4.3 cm plot	= 1548 characters
Figure 2	18 cm x 11 cm plot	= 3960 characters
Figure 3	18 cm x 6 cm plot	= 2016 characters
Table 1	12 lines x 8.7 cm	= 720 characters

Abstract

Since 1980, the number of undernourished people in eastern and southern Africa has more than doubled. Rural development stalled and rural poverty expanded during the 1990s. Population growth remains very high and declining per capita agricultural capacity retards progress towards Millennium Development goals. Analyses of in situ station data and satellite observations of precipitation identify another problematic trend. Main growing season rainfall receipts have diminished by ~15% in food insecure countries clustered along the western rim of the Indian Ocean. Occurring during the main growing seasons in poor countries dependent on rain fed agriculture, these declines are societally dangerous. Will they persist or intensify? Tracing moisture deficits upstream to an anthropogenically warming Indian Ocean leads us to conclude that further rainfall declines are likely. We present analyses suggesting that warming in the central Indian Ocean disrupts onshore moisture transports, reducing continental rainfall. Thus late 20th century anthropogenic Indian Ocean warming has probably already produced societally dangerous climate change by creating drought and social disruption in some of the world's most fragile food economies. We quantify the potential impacts of the observed precipitation and agricultural capacity trends by modeling millions undernourished people as a function of rainfall, population, cultivated area, seed and fertilizer use. Persistence of current tendencies may result in a 50% increase in undernourished people. On the other hand, modest increases in per capita agricultural productivity could more than offset the observed precipitation declines. Investing in agricultural development can help mitigate climate change while decreasing rural poverty and vulnerability.

Text

Introduction – food insecurity along Africa's eastern coast

Sustainability science often looks at trends and the interaction of trends(1, 2) through the lens of 'use-inspired basic research'(1). We present here an analysis of rainfall and agricultural capacity trends inspired by our research supporting earlier early warning for the US Agency for International Development's Famine Early Warning System (Table S1). Most of this work has focused on monitoring and predicting emerging drought conditions in Eastern and Southern Africa(3-5), one way of improving adaptive capacity(6) recommended by the Intergovernmental Panel on Climate Change (IPCC). In 2003, however, a routine attempt to use early season rainfall (March-April) rainfall as a predictor of late season (September-October) crop production produced a disturbing discovery. Substantial rainfall declines had occurred within critical crop growing areas in Ethiopia. The place and timing of these trends made them dangerous. Further analysis suggested links to drought across much of eastern eastern Africa during the long rains season, and potential anthropogenic links to the central Indian Ocean(3, 5). In addition to climate analysis, this work also included evaluations of population, agriculture and water security. We find that in eastern and southern Africa, the combination of declining per capita agricultural capacity(7) and increasing aridity is exacerbating vulnerability(8) and rural poverty(9). Declining investments in rural development, rapidly increasing rural populations, the depletion of soil nutrients through erosion, and the cultivation of most cultivatable areas limit agricultural productivity growth(10). Low per capita agricultural production and rural poverty go hand in hand, slowing progress towards Millennium Development Goals (MDGs). A recent overview of these goals(11) indicates differential progress on different fronts. Education and economic conditions have improved. Population growth remains high (2.3 percent a year). Progress on hunger and health has been halting. Our concern is that post-1980 rainfall declines during the main eastern African long rains (March to May) and the main southern African summer rains (December to February) may be contributing to African food insecurity. We believe that these declines may be associated with anthropogenic warming in the Indian Ocean. If so, these precipitation declines, acting in concert with declining agricultural capacity, likely constitute a prime example of societally dangerous climate change.

In this report we quantify the likely impact of observed precipitation and agricultural capacity trends using empirical food balance indicator models. These models estimate the millions of undernourished people as a function of population, cropped area, seed use, fertilizer applications, and main growing season precipitation. These models show that continued declines in rainfall and per capita agricultural capacity will produce increasing food insecurity. We next use observations and climate model simulations to argue that recent declines in eastern and southern African growing season rainfall are linked to anthropogenic warming in the Indian Ocean. This link to global warming implies that these precipitation declines are likely to continue or intensify. For eastern Africa, this result is at odds with the most recent IPCC assessment(12, 13), which anticipates precipitation increases. For southern Africa, this result is consistent with previous analyses(13, 14), which anticipate rainfall declines. We are essentially arguing that warming in the south-central Indian Ocean (0-15°S, 60-90°E) has a similar effect on near coastal eastern and southern Africa during boreal winter and spring. In each season, oceanic warming appears to reduce onshore moisture transports(5, 15-17) while increasing continental atmospheric stability.

This may explain recent drought tendencies in gauge data, satellite-observed precipitation*, lake levels(5, 16) and vegetation indices in densely populated water-insecure regions of eastern African. If a common anthropogenic Walker-cell like disruption has caused declines in both southern and eastern African rainfall, then this disruption is likely to persist. Furthermore, recent climate change impact assessments(18), based on optimistic precipitation simulations over eastern Africa, may underestimate yield reductions(4). Our food balance modeling of millions of undernourished, however, suggests that these impacts could be mitigated by agricultural development.

Modeling the impacts of agricultural capacity and rainfall

Over the past 25 years the population of food insecure eastern and southern Africa has doubled while per capita cropped area has declined by 33% and the millions of undernourished increased by 80%(19). Today, one out of three small children is dangerously underweight and 40% of 308 million people are undernourished. Average national per capita cropped area values are often below 1,000 m^2 per person†. Food aid has become chronic, with 2005 World Food Programme (WFP) aid valued at $200US million. Poor farmers in these countries, often trapped in cycles of displacement, division and degradation(20), depend on rainfed agriculture(21). Per capita crop production is an important metric of food availability and security. Limited technological inputs create a strong dependence between national average cropped area and national average production (r=0.95).

Recent agricultural capacity trends tend to be dominated by cropped area and population growth increases*. In general, increased food production has matched growing population through increased labor inputs and through extensification, with area under cultivation increasing by 50% over the past 25 years while population has almost doubled (Fig. 1.A). Seed and fertilizer use has also lagged population growth. Unfortunately, since 1990, overseas agricultural assistance has declined from 12 to 4% of total foreign aid(7), and only 4% of African public spending goes to agriculture(7). This has contributed to stalling increases in agricultural inputs. As the gap between population growth and structural agricultural components continues to grow, vulnerability and rural poverty will increase, amplifying the impact of agricultural droughts. These droughts appear to be more severe in recent years (Fig. 1.A), and main growing season rainfall* has declined by about 15% across Eastern and Southern Africa, in step with recent increases in radiative forcing(22). The interaction of agricultural and rainfall trends may be represented by empirical models estimating the millions of undernourished people.

The five components of national per capita production (rainfall, population, cropped area, seed and fertilizer use) can be combined into two variables: rainfall and per capita agricultural capacity. Agricultural capacity represents the slowly varying non-weather component of a national food balance, and is a function of cropped area, seeds and fertilizer divided by population with units of per capita crop production [kg $person^{-1}$ $year^{-1}$]. Fig. 1.B shows main growing season rainfall and per capita agricultural capacity trends for ten eastern and southern African nations. Somalia has been excluded due to limited data. Downward point arrows (Ethiopia, Kenya, Burundi, Tanzania,

* Please see our online supporting materials for a specific description of our methods.

† Agriculture, population, food security and food aid statistics were obtained from the UN Food and Agriculture Organization (FAO)

Malawi, Zambia, Zimbabwe) indicate countries experiencing key growing season rainfall declines between 1979 and 2005. Note the geographic clustering of observed rainfall declines along Africa's eastern seaboard. Countries with left pointing vectors (Ethiopia, Uganda, Zambia, Zimbawbe) have experienced 1994-2003 declines.

In these semi-arid countries a strong dependence on rain-fed smallholder farming practices results in quasi-linear relationships between grain yields, seasonal rainfall receipts, and food deficits. Hence, agricultural capacity multiplied by percent normal rainfall is strongly related to per capita production. The inverse of this measure (food imbalance) is related to food aid[*]. For each country (except Ethiopia, due to data limitations), the food imbalance measure was regressed against 'millions of undernourished' statistics obtained from the United Nations' Food and Agriculture Organization. This gives us a pragmatic means of translating changes in rainfall, cropped area, seed and fertilizer use into an index of food insecurity, grounded empirically by historic observations. The resulting model performed well at a national/inter-annual scale for eastern and southern Africa ($r=0.86$, $p=1.6\times10^{-5}$). In order to stress the semi-quantitative nature of these projections, we present our results as percent changes from a 2000 baseline. This also allows comparison with the Millenium Development goal of halving the number of undernourished by 2015.

Three scenarios were examined (Fig. 1.C). Scenario 1 represents a 'business as usual' future. Recent precipitation and agricultural capacity trends were assumed to persist through 2030. Under this scenario, the aggregate tendencies shown in Fig. 1.A continue, and undernourishment increases by 53% between 2000 and 2030. The effects of agricultural capacity declines alone can be seen in Scenario 2. Undernourishment increases by 23%. On the other hand, evaluating a combination of observed rainfall declines paired with moderate increases in per capita agricultural capacity of two kilograms per person per year, equivalent to a 2% per capita growth rate, exhibited substantial (38%) declines in undernourishment. Drought interacts dangerously with low agricultural capacity, but its effects can be mitigated through agricultural development.

Walker cell-like anomalies may explain observed rainfall declines

Will the observed rainfall declines (Fig. 1) persist, increasing levels of undernourishment (Fig. 1.C)? Fueling this concern is the strong covariance between global temperatures ($r=0.82$) and south-central Indian Ocean (0-15°S, 60-90°E) sea surface temperatures (SSTs). Both have risen dramatically since the 1980s, along with radiative forcing (Fig. 2.A), and tropical Indian Ocean SSTs recently reached their highest value in 120,000 years(23). While anthropogenic warming has occurred in all oceans(24), this warming has been larger in the Indian Ocean(25). Recent careful analysis identifies an 0.5-1.0°C 1960-1999 SST increase in the Indian Ocean Thermal Archive(26). This study also finds that most (7 out of 10) World Climate Research Programme Coupled Model Intercomparison Project(27) (CMIP3) models recreate this tropical warming tendency, strongly implicating greenhouse gas and aerosols emissions in the recent observed warming (Fig. 2.D). Modelled CMIP3 increases in southern tropical Indian Ocean temperatures are strongly linked to trends in equatorial Pacific zonal wind stress and southward shifts in the latitudinal position of the subtropical gyre. Warmer oceanic SSTs have produced substantial increases in precipitation over the tropical Indian Ocean, indicated by both satellite(28) (13%) and reanalysis(29) (28%) datasets. This convection releases energy in the atmosphere, influencing the

regional weather via a Walker cell-like circulation anomaly. This mechanism may have been responsible for the 1984 Ethiopian drought(30).

The statistical connection between increased oceanic precipitation and continental rainfall is shown in Fig. 2.B*. Both data sources have been normalized, hence a regression coefficient of -0.6 associates a one standard deviation increase in oceanic precipitation with a -0.6 standard deviation decrease in African rainfall. The latitude of negative associations shifts with the march of seasons, following the thermal equator and path of maximum onshore moisture transports (shown schematically with arrows).

The connection between seasonal moisture transports and central Indian Ocean warming (represented by precipitation) can be explored empirically via canonical correlation analysis (CCA). CCA is a statistical technique that finds dominant patterns of covariability in two sets of multivariate data. The two sets of data examined were seasonal 1950-2005 zonal reanalysis moisture transports over Africa's eastern seaboard (20°N-20°S, 25°E-45°E) and seasonal tropical Indian Ocean precipitation (15°N-15°S, 55°E-90°E). Tropical oceanic precipitation is linearly related to diabatic atmospheric heating, which can produce east-west Walker cell-like circulations anomalies(31). Our hypothesis is that these anomalous circulations control decadal rainfall fluctuations endangering food insecure Africa.

Fig. 2.C shows our CCA results for March-April-May (other seasons are presented in Fig. S1). In each season, we find that the 1st canonical correlate identifies a 1st CCA pattern describing shared Indian Ocean precipitation and moisture transport variations. This approach produces time-series describing covariant Indian Ocean precipitation (CC_P) and moisture transports (CC_M). Increasing tropical Indian Ocean precipitation (blue circles) is associated with atmospheric ridging and anti-cyclonic moisture circulations over eastern Africa (arrows). This disrupts the main onshore moisture flows (shown with blue shading). University of Delaware precipitation deficits for the strongest six oceanic precipitation events are shown with red boxes. While only boreal spring results are shown here, the patterns for other seasons are similar; a Walker cell-like dipole emerges as the dominant (1st canonical correlate) relationship. The transport correlations indicate reduced onshore moisture fluxes between 0 and 15°S. This region supplies 66% of Indian Ocean-sourced zonal moisture transports into Tropical Africa, and 83% of the annual mean zonal moisture transports entering tropical Africa originate in the Indian Ocean. The northern flanks of the CCA patterns are associated with transport anomalies flowing from the drier Sahelian regions. Thus changes in central Indian Ocean precipitation are correlated with transitions between dry continental and moist oceanic air masses over tropical Africa.

At low (decadal) frequencies, correlations between the CC_M and CC_P approach unity, and the zonal transport indices are negatively correlated (r~-0.9) with regional rainfall (Table 1). In total the CCA-identified transports can explain 85% of the low frequency variations in eastern MAM, southern DJF and Sahelian JJA rainfall. All three seasons/regions experienced a 1960-1970 decline in observed rainfall and CCA transport forcing, in synch with anthropogenic 1960-1970 increases in Indian Ocean heat content(24-26). A second heat content increase in the early 1980s was associated with MAM and DJF transport disruptions and drying tendencies in southern and eastern Africa. Slower increases in JJA transport disruptions, combined with north/south shifts in Atlantic

sea surface temperatures (SSTs), has likely led to a modest recovery in Sahelian rainfall(14, 32), albeit with continued declines across the eastern Sahel and southern Ethiopia(32).

To examine the influence of diabatic heating on moisture transports in a simulation framework, we have also conducted experiments with the NCAR CAM*, a fully non-linear atmospheric model with explicitly resolved moist processes. An additional diabatic heating term is added over the central Indian Ocean, which increases the local rainfall, as in Barlow et al(33). The added heating is sinusoidal in latitude and longitude for a half period over the domain -20° S to 5°N and 50 to 100°E with a magnitude of 0.02 $W\,kg^{-1}$. This southern central Indian Ocean domain was chosen to match our previous observational analyses(5, 16) and the early assertion that enhanced cyclonic activity helped create the tragic 1984 Ethiopian Famine(30). A clear influence on moisture transport over the interior of Africa is observed (Fig. 2.D), in good agreement with the expectations of simple Gill-type dynamics, and is associated with decreases in local rainfall. These MAM circulation anomalies are similar to previous modeling results for JFM(17), and the observed low-level circulation anomalies associated with warm Indian Ocean warming seasons for boreal spring (Fig. 2.C). Thus while the relevance of the simple Gill model might be questioned, especially as it neglects the mean wind(34), the general link between increased central Indian Ocean precipitation and decreased onshore moisture transport appears robust even in a full atmospheric model.

In summary, the strong, probably anthropogenic(24-26) warming of the south-central Indian Ocean (Fig. 2.A), increases maritime precipitation, which is statistically and dynamically related to continental rainfall declines and moisture transport reductions (Figs. 2B, 2C). Non-linear climate simulations driven by diabatic heating over the Indian Ocean produce similar transport anomalies (Fig. 2.D and ref. (17)). In this context, what do projected 21st climate changes suggest over the Indian Ocean and tropical Africa?

Climate change simulations suggest continued Indian Ocean Warming

In this section we present a multi-model analysis of CMIP3 precipitation simulations. If the consensus of these models suggests continued increases in oceanic precipitation, then we should be concerned that continued continental rainfall declines, similar to those shown in Fig. 2B, will lead to increased undernourishment unless mitigated (Fig. 1.C). We selected 11 models having both 20th century (20c3m) and 21st century climate simulations. Because near-term (2000-2030) projections of radiative forcing(22) are quite similar across the various emission projections(35), the various 21st century scenarios were combined. Figure 3 summarizes results for the critical March-April-May east African growing season*. December-January-February results were similar and are not shown.

We begin by analyzing east-west (zonal) tropical precipitation tendencies. Panel 3.A shows a time-longitude plot of temporal z-scores (standard deviations, σ) of the CMIP3 ensemble means averaged between 15°N/S. In this plot the 1950-2100 MAM multi-model means were averaged between 15°N and 15°S at 5° intervals between 20°E and 160°E. The time-series at each longitude was translated into z-scores (standard deviations) and plotted with red (blue) indicating reduced (enhanced) precipitation. As greenhouse gas forcing increases with time, beginning in the 1970s, precipitation increases across the Indian Ocean and declines across tropical Africa. This timing is

broadly consistent with observed increases in oceanic SSTs (Figure 2.A) and reductions in continental rainfall (Fig. 1.A). We can analyze scatter surrounding the CMIP3 climate change consensus by translating the 132 individual precipitation simulations into time-varying probability distribution functions[*],(36) (pdfs). Fig. 3.B shows the multi-model ensemble precipitation pdfs over the tropical Indian Ocean (0-15°S, 60-90°E). As greenhouse gasses and aerosols accumulate in the atmosphere, the Indian Ocean warms, oceanic precipitation increases, presumably producing moisture transport variations and tropical African rainfall declines similar to those shown in Fig. 2. The pdfs are tight and trend strongly, increasing steeply after the mid 1970s, in step with radiative forcing increases(22) and observed African rainfall declines (Fig. 1) so that by late in the 21st Century the ranges of precipitation projected are quite different from historical ranges. Panel 3.C shows Indian Ocean precipitation changes for the eleven different individual models (x axis) along with the correlation between each model's multi-simulation mean time-series and the ensemble mean (y). All models exhibit positive correlations, so that the models were unanimous in projecting increases in March-April-May atmospheric warming (i.e. precipitation) over the tropical Indian Ocean. The frequency with which MAM central Indian Ocean precipitation totals in 2031-2050 exceeded the average rainfall total for 1951-1970 increased by more than 20% in 10 of the 11 models. Taken together the panels of Fig 3 indicate tilt of the odds towards more precipitation over the Indian Ocean and less precipitation over Africa's eastern seaboard.

Summary and Conclusions

Two independent, but interacting, post-1980 tendencies have contributed to food insecurity in eastern and southern Africa (Fig. 1). First, population growth has exceeded increases in agricultural infrastructure and cultivated area. Second, there has been a tendency for main growing season rainfall to decline. Empirical and model-based explorations (Fig. 2, S2) support assertions that Walker-cell-like disruptions to of atmospheric circulations and moisture transports link a warming Indian Ocean to a drier eastern African seaboard. Multi-model CMIP3 ensembles (Fig. 3 and ref (17)) suggest greenhouse gas and aerosols emissions have contributed substantially to this observed late twentieth century warming (Fig. 2.A). Anthropogenic climate change has probably produced societally dangerous increases in eastern and southern African food security. These conclusions, in general, agree with the most recent 4th Intergovernmental on Panel on Climate Change (IPCC) finding that semi-arid Africa may experience large scale water-stress(37) and yield reductions(18) by 2030.

The results presented here, however, differ in approach from the IPCC models, focusing on empirical relationships rather than raw CMIP3 precipitation simulations. These raw simulations have implied that eastern Africa might become wetter while southern Africa becomes drier[30]. We question the fidelity, in general, of continental precipitation simulations, especially over the extremely complex terrain of east Africa. Global models suppress important local mechanisms (internal thermal and orographic gravity waves[31]), and vary substantially in their ability to represent the transient systems that draw kinetic energy from the mean circulation, overcoming stability inhibitions and producing organized mesoscale convection[32]. Even monthly reanalysis precipitation fields have almost no skill (R^2<0.2) when compared with observations in eastern Africa. Given this uncertainty, we believe that the observed quasi-linear negative relationships between central Indian Ocean warming and east African rainfall represents the mostly likely outcome. This may be indicative of other 'Indian Rim' and South American countries as well,

since similar precipitation reformulations also suggest main season declines(38), with the result that main growing season droughts may disproportionately affect tropical and sub-tropical countries. Global assessments of anthropogenic precipitation(13) and yield(18) changes may be underestimating these drought signals. The climate change impacts in low-income nations have been almost completely driven by emissions from middle and high income countries(39). While more research, and better climate models, will be required to settle quantitatively issues of attribution, the social and economic disruptions associated with anthropogenic drought may add substantially to these impacts.

Vulnerability arises through a complex interplay of exposures, sensitivities, and resiliencies that can either dampen or amplify the impact of climatic shocks(8). The recent IPCC assessment identifies many means of enhancing adaptive capacity(6) in Africa. Improved forecasts and earlier early warning can help(4), as can improving existing rain-fed agriculture through farm managment(40) (Cf. Table 2 in Ref (6)), as can enhanced bio-technological(41) inputs. Recent research suggests that investments in African agricultural development will lead to substantial pro-poor economic growth(41-43). The continuation of recent tendencies will be likely to result in continued increases in undernourishment. This is not a *fait accompli*. The range of possible human outcomes is large, and depends largely on the choices that we make. By 2025 rates of child malnutrition, for example, could range from 9.4 to 41.9 million(44). Our food aid models suggest that a 15% increase in yields per decade (equivalent to a 2 kg per person per year increase in agricultural capacity) could come close to achieving the MDG of halving the number of undernourished, albeit by 2030 rather than 2015.

While notable achievements in economic growth and education have been made since 1999, recent progress on hunger in Africa has been very slow(11) and has fallen short of keeping pace with the relatively rapid population growth. The past few years have seen an increased governmental appreciation of the role of agricultural development(7), but public investments in agriculture and international donor assistance have lagged behind MDG commitments(11). More and higher quality assistance and agricultural polices, guided by objective policy design and better governance, can help eastern and southern Africa achieve sustainability transition. Investments in agricultural capacity seem warranted, given the large financial and humanitarian costs of business as usual in a changing climate system. These investments may also be just, given the strong evidence for anthropogenic drought and the disproportionate emissions by middle and high income countries(39).

Acknowledgments

This research was supported by USAID* under a USGS cooperative agreement (04HQAG0001) and by NASA under a precipitation science grant (NNX07AG26G). We would like to these agencies for their support. We would also like to thank and acknowledge the CMIP3 modeling groups for providing their data for analysis, the Program for Climate Model Diagnosis and Intercomparison (PCMDI) for collecting and archiving the model output, and the JSC/CLIVAR Working Group on Coupled Modeling (WGCM) for organizing the model data analysis activity. The multi-model data archive is supported by the Office of Science, U.S. Department of Energy.

Figure legends

Fig. 1. Food security analysis. A. Rainfall, population, cropped area, seed use and fertilizer use for eastern and southern Africa. Rainfall is expressed as a percent of the 1951-1980 average. The other variables are expressed as percents of 1979-1981 averages. Global radiative forcing is shown with a stippled line on an inverted axis. **B.** The black vectors denote recent observed rainfall and agricultural capacity tendencies. Agricultural data were obtained from the Food and Agriculture Organization. **C.** Empirical food balance models results, expressed as percentages of 2000 undernourishment.
Size: 2 column (18 cm x 4.3 cm)

Fig. 2. A. time-series of GISS global temperatures and Kaplan Indian Ocean SSTs. **B.** Pixel-by-pixel bivariate regressions coefficients for seasonal standardized precipitation indices. For each season standardized southwest Indian Ocean (SWIO) GPCP precipitation. The red arrows show the general location of lower tropospheric (850 hPa) westward wind maxima. **C.** First canonical correlates for each season. Results have been screened for significance ($p < 0.1$). The blue shading denotes the core of the westward transports, with mean 850 hPa wind speeds of greater than 4 ms^{-1}. **D.** CAM diabatic forcing expirement results. Arrows indicate simulated moisture transport anomalies [$kg\ kg^{-1} ms^{-1}$]. Blue-red shading indicates diabatic heating anomalies [$K\ day^{-1}$].

Size: 2 columns (18 cm x 11 cm)

Fig 3. **CMIP3 March-April-May precipitation simulation results. A.** A time (1950-2100) versus longitude plot of CMIP3 ensemble means averaged between 15°N/S. At each 5° longitude box the 150 years of precipitation values were translated into z-scores (standard deviations, σ). Red shades indicate drier conditions. Blue shades indicate above normal precipitation. **B.** A time versus probability plot showing the multi-model ensemble pdfs[29] for the south-central Indian Ocean (0-15°S, 60-90°E). **C.** Summary of changes in frequency of above "normal" precipitation and correlation of precipitation changes in individual climate models with the multi-model ensemble means for this same region.
Size: 2 columns (18 cm x 6 cm)

1

References

1. Clark WC (2007) *Proc. Nat. Acad. Sci.* **104,** 1737-1738.
2. Kates RW & Parris TM (2003) *Proc. Nat. Acad. Sci.* **100,** 8062-8067.
3. Funk C, Senay G, Asfaw A, Verdin J, Rowland J, Michaelsen J, Eilerts G, Korecha D, & Choularton R (2005) in *Famine Early Warning System Network Special Report* (USAID).
4. Brown ME, Funk CC, Galu G, & Choularton R (2007) *EOS, Transactions American Geophysical Union* **88,** 381-382.
5. Verdin J, Funk C, Senay G, & Choularton R (2005) *Philosophical Transactions of Biological Sciences* **360,** 2155-2168.
6. Boko M, Niang I, Nyong A, Vogel C, Githeko A, Medany M, Osman-Elasha B, Tabo R, & Yanda P (2007) in *Climate Change 2007: Impacts, Adaptation and Vulnerability. Contribution of Working Group II to the Fourth Assessment Report of the Intergovernmental Panel on Climate Change*, eds. Parry ML, Canziani OF, Palutikof JP, van der Linden PJ, & Hanson CE (Cambridge University Press, Cambridge UK), pp. 433-467.
7. WorldBank (2008) *World Development Report 2008: Agriculture for Development* (The International Bank for Reconstruction and Development / The World Bank).
8. Turner BL, Kasperson RE, Matson PA, McCarthy JJ, Corell RW, Christensen L, Eckley N, Kasperson JX, Luers A, Martello ML, *et al.* (2003) *Proc. Nat. Acad. Sci.* **100,** 8074.
9. OXFAM (2006) *OXFAM briefing paper*.
10. Kates RW & Parris TM (2003) *Proc. Nat. Acad. Sci.* **100,** 8062-8067.
11. UN (2007) (United Nations Department of Public Information).
12. Christensen JH, B. Hewitson, A. Busuioc, A. Chen, X. Gao, I. Held, R. Jones, R.K. Kolli, W.-T. Kwon, R. Laprise, *et al.* (2007), eds. Solomon S, Qin D, Manning M, Chen Z, Marquis M, Averyt KB, Tignor M, & Miller HL (Cambridge University Press, Cambridge, UK and New York, NY).
13. Solomon S, Qin D, Manning M, Chen Z, Marquis M, Averyt KB, Tignor M, & Miller HL (2007) *Climate change 2007: the physical science basis. Contribution of working group I to the fourth assessment report of the Intergovernmental Panel on Climate Change.* (Cambridge University Press, Cambridge, UK).
14. Hoerling M, Hurrell J, Eischeid J, & Phillips A (2006) *Journal of Climate* **19,** 3989-4008.
15. Cook KH (2000) *Journal of Climate* **13,** 3789-3804.
16. Funk C, Senay G, Asfaw A, Verdin J, Rowland J, Michaelsen J, Eilerts G, Korecha D, & Choularton R (2005) (USAID Famine Early Warning System Network).
17. Washington R & Preston A (2006) *Journal of Geophysical Research* **111,** D15104.
18. Lobell DB, Burke MB, Tebaldi C, Mastrandrea MD, Falcon WP, & Naylor RL (2008) *Science* **319,** 607-610.
19. FAO (2006) (Food and Agriculture Organization of the United Nations).
20. Kates RW (2000) *Climatic Change* **45,** 5-17.
21. Rockstrom J (2000) *Physics and Chemistry of the Earth Part B: Hydrology, Oceans and Atmosphere* **25,** 275-283.
22. Forster P, Ramaswamy V, Artaxo P, Berntsen T, Betts R, Fahey DW, Haywood J, Lean J, Lowe DC, Myhre G, *et al.* (2007) in *Climate Change 2007: The Physical Science Basis. Contribution of Working Group I to the Fourth Assessment Report of the Intergovernmental Panel on Climate Change*, eds. Solomon S, Qin D, Manning M, Chen

Z, Marquis M, Averyt KB, Tignor M, & Miller HL (Cambridge UniversityPress, Cambridge, United Kingdom and New York, NY, USA.).
23. Hansen J, Sato M, Ruedy R, Lo K, Lea DW, & Medina-Elizade M (2006) *Proceedings of the National Academy of Sciences of the United States of America* **103,** 14288-14293.
24. Barnett TP, Pierce DW, & Schnur R (2001) *Science* **292,** 270-274.
25. Cai W, Cowan T, Dix M, Rotstayn L, Ribbe J, Shi G, & Wijffels S (2007) *Geophysical Research Letters* **34,** L14611.
26. Alory G, Wijffels S, & Meyers G (2007) *Geophysical Research Letters* **34,** L02606.
27. Meehl GA, Covey C, Delworth T, Latif M, McAvaney B, Mitchell JFB, Stouffer RJ, & Taylor KE (2007) *Bulletin of the American Meteorological Society* **88,** 1383-1394.
28. Adler RF, Huffman GJ, Chang A, Ferraro R, Xie P-P, Janowiak J, Rudolf B, Schneider U, Curtis S, Bolvin D, *et al.* (2003) *Journal of Hydrometeorology* **4,** 1147-1167.
29. Kalnay E, Kanamitsu M, Kistler R, Collins W, Deaven D, Gandin L, Iredell M, Saha S, White G, Woollen J, *et al.* (1996) *Bulletin of the American Meteorological Society* **77,** 437-471.
30. Shanko D & Camberlin D (1998) *Int. J. of Climatol.* **18,** 1373–1388.
31. Gill A (1982) *Atmosphere-Ocean Dynamics* (Academic Press, UK).
32. Held IM, Delworth TL, Lu J, Findell KL, & Knutson TR (2005) *Proceedings of the National Academy of Sciences* **102,** 17891-17896.
33. Barlow M, Hoell A, & Colby F (2007) *Geo. Res. Let.* **34,** L19702,doi:19710.11029/12007GL030043.
34. Ting M & Sardeshmukh P (1993) *J. Atmos. Sci.* **34,** 280-296.
35. Dai A, Wigley TML, Boville BA, Kiehl JT, & Buja LE (2001) *Journal of Climate* **14,** 485-519.
36. Dettinger M (2006) *Climatic Change* **76,** 149-168.
37. Easterling W, Aggarwal P, Batima P, Brander K, Erda L, Howden M, Kirilenko A, Morton J, Soussana JF, Schmidhuber S, *et al.* (2007) in *Climate Change 2007: Impacts, Adaptation and Vulnerability. Contribution of Working Group II to the Fourth Assessment Report of the Intergovernmental Panel on Climate Change*, eds. Parry ML, Canziani OF, Palutikof JP, van der Linden PJ, & Hanson CE (Cambridge University Press, Cambridge), pp. 273-313.
38. Brown ME & Funk C, C. (2008) *Science* **319,** 580-581.
39. Srinivasana UT, Carey SP, Hallsteind E, Higginsd PAT, Kerrd AC, Koteend LE, Smith AB, Watson R, Hartec J, & Norgaardd RB (2008) *Proc. Nat. Acad. Sci.* **105,** 1768-1773.
40. Rockström J (2003) *Phys. Chem. Earth* **28,** 869-877.
41. Delmer DP (2005) *Proc. Nat. Acad. Sci.* **102,** 15739
42. Thirtle C, Lin L, & Piesse J (2003) *World Development* **31,** 1959-1975.
43. Tiffin R & Xavier I (2006) *Agricultural Economics* **35,** 79–89.
44. Rosegrant MW, Cline SA, Weibo L, Sulser TB, & Valmonte-Santos RA (2005) (International Food Policy Research Institute).

A. Indian Ocean sea surface temperatures and global surface temperatures tightly coupled and rising steeply since 1980

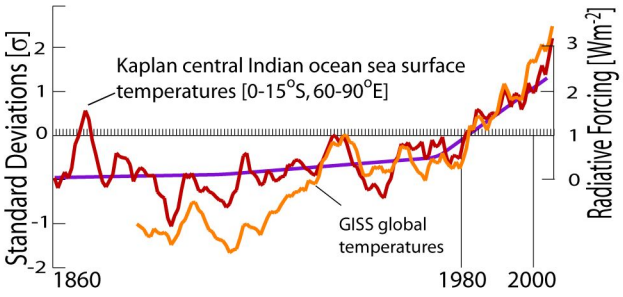

B. Regressions show negative relationships between growing season rainfall and Indian Ocean precipitation

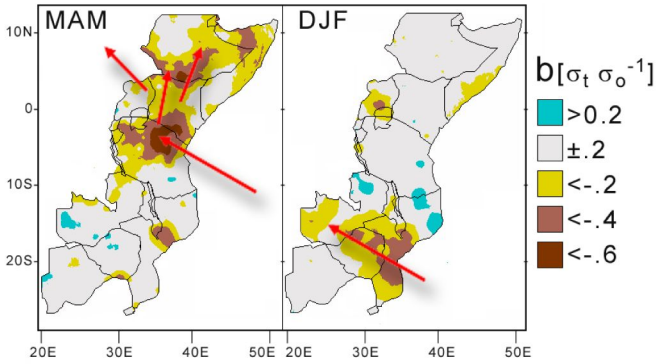

C. Canonical correlations link increasing oceanic precipitation with moisture transport disruptions

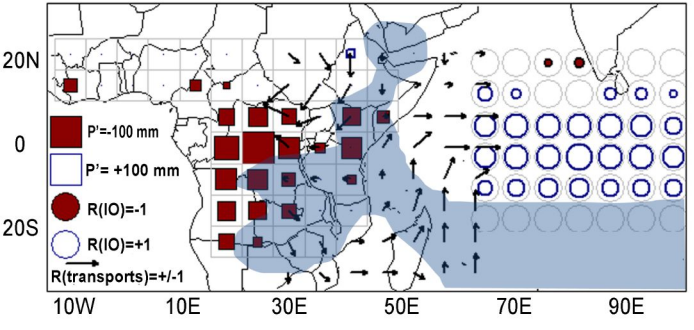

D. CAM diabatic forcing experiment results produce eastward moisture transports

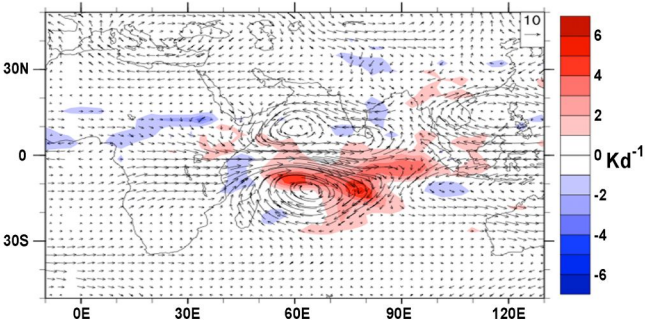

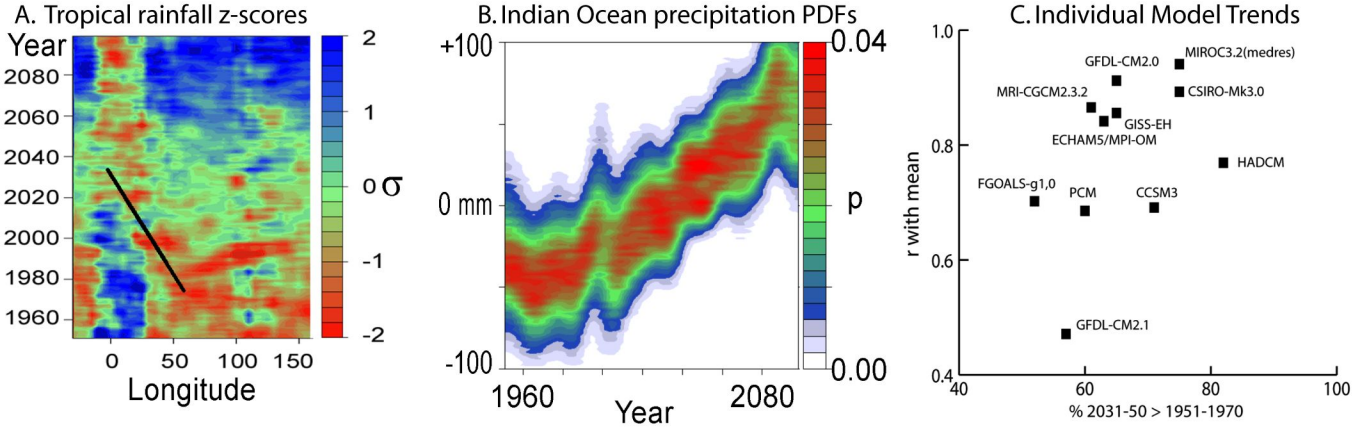
A. Tropical rainfall z-scores
Year
2080
2060
2040
2020
2000
1980
1960
0
50
100
150
Longitude
2
1
0 σ
-1
-2
B. Indian Ocean precipitation PDFs
+100
0 mm
-100
1960
Year
2080
0.04
p
0.00
C. Individual Model Trends
1.0
0.8
0.6
0.4
r with mean
40
60
80
100
% 2031-50 > 1951-1970
MIROC3.2(medres)
GFDL-CM2.0
CSIRO-Mk3.0
MRI-CGCM2.3.2
GISS-EH
ECHAM5/MPI-OM
HADCM
FGOALS-g1,0
PCM
CCSM3
GFDL-CM2.1

Table 1. Correlations between climate, rainfall and food security indices

	DJF R (p-value)	**MAM** R (p-value)	**JJA** R (p-value)
CC_P & CC_U			
Inter-annual (1950-05)	0.45 (5.6×10^{-4})	0.81 (6.5×10^{-14})	0.64 (1.4×10^{-8})
7-year timescale (1950-05)	0.90 (2.3×10^{-3})	0.97 (6.6×10^{-5})	0.90 (2.3×10^{-3})
CC_U & growing season rainfall	Southern Africa	Eastern Africa	Sahel countries
Inter-annual (1950-05)	-0.39 (3.2×10^{-3})	-0.50 (1.0×10^{-4})	-0.57 (2.7×10^{-5})
7-year timescale (1950-05)	-0.82 (4.6×10^{-2})	-0.92 (9.3×10^{-3})	-0.92 (9.3×10^{-3})
CC_P & CMIP3 oceanic rainfall			
7-year timescale (1966-05)	0.97 (1.2×10^{-3})	0.91 (1.6×10^{-2})	0.86 (2.8×10^{-2})
CC_P & Global Temperature			
7-year timescale (1966-05)	0.88 (2.0×10^{-2})	0.85 (3.2×10^{-2})	0.84 (3.6×10^{-2})